The mouse organellar biogenesis mutant buff results from a mutation in *Vps33a*, a homologue of yeast *vps33* and *Drosophila* carnation

Tamio Suzuki*†‡, Naoki Oiso*†, Rashi Gautam†§, Edward K. Novak§, Jean-Jacques Panthier¶, P. G. Suprabha‖, Thomas Vida, Richard T. Swank§, and Richard A. Spritz*††**

*Human Medical Genetics Program, University of Colorado Health Sciences Center, Denver, CO 80262; §Department of Molecular and Cellular Biology, Roswell Park Cancer Institute, Buffalo, NY 14263; ¶Institut National de la Recherche Agronomique, Ecole Nationale Vétérinaire d'Alfort, 94704 Maisons-Alfort Cedex, France; ‖Center for Basic Neuroscience, University of Texas Southwestern, Dallas, TX 75390; and **Department of Microbiology and Molecular Genetics, University of Texas Medical School, Houston, TX 77030

Communicated by Theodore T. Puck, Eleanor Roosevelt Institute for Cancer Research, Denver, CO, December 2, 2002 (received for review July 16, 2002)

In the mouse, more than 16 loci are associated with mutant phenotypes that include defective pigmentation, aberrant targeting of lysosomal enzymes, prolonged bleeding, and immunodeficiency, the result of defective biogenesis of cytoplasmic organelles: melanosomes, lysosomes, and various storage granules. Many of these mouse mutants are homologous to the human Hermansky–Pudlak syndrome (HPS), Chediak–Higashi syndrome, and Griscelli syndrome. We have mapped and positionally cloned one of these mouse loci, buff (*bf*), which has a mutant phenotype similar to that of human HPS. Mouse *bf* results from a mutation in *Vps33a* and thus is homologous to the yeast vacuolar protein-sorting mutant *vps33* and *Drosophila* carnation (*car*). This is the first found defect of the class C vacuole/prevacuole-associated target soluble *N*-ethylmaleimide-sensitive factor attachment protein receptor (t-SNARE) complex in mammals and the first mammalian mutant found that is directly homologous to a *vps* mutation of yeast. *VPS33A* thus is a good candidate gene for a previously uncharacterized form of human HPS.

Hermansky–Pudlak syndrome (HPS) is a disorder of organelle biogenesis in which oculocutaneous albinism, bleeding, and in most cases pulmonary fibrosis result from defects of melanosomes, platelet-dense granules, and lysosomes (1–4). Somewhat similar disorders, Chediak–Higashi and Griscelli syndromes, are additionally associated with severe immunodeficiency (2, 3). Important clues to the pathogenesis of these disorders have come from the mouse, in which >16 loci have been associated with mutant phenotypes similar to those of human HPS, Chediak–Higashi syndrome, and Griscelli syndrome (5, 6). Several of these genes have been identified recently and in a number of cases have been shown to result in homologous disorders in mice and humans (2–4). Although the functions of many of the corresponding gene products remain unknown, several are involved in various aspects of trafficking proteins to nascent organelles, particularly melanosomes, lysosomes, and cytoplasmic granules. In the yeast, >65 proteins have been implicated in biogenesis of the cytoplasmic vacuole, including the products of >40 vacuolar protein-sorting (*vps*) loci required for trafficking newly synthesized proteins from the late Golgi/*trans*-Golgi network to the vacuole (7, 8). It seems likely that at least as many proteins are associated with organellar biogenesis in mammals.

We have mapped and positionally cloned the mouse buff (*bf*) locus, which is characterized by recessive coat-color hypopigmentation and mild platelet-storage pool deficiency but has little if any effect on lysosomal function. We find that mouse *bf* results from a missense substitution in *Vps33a*, a homologue of yeast *vps33*. The *bf* mutation results in defective melanosome morphology and melanogenesis both *in vivo* and *in vitro*. Expression of wild-type *Vps33a* in transfected mouse *bf*-mutant melanocytes complements this aberrant phenotype, whereas expression of *bf*-mutant *Vps33a* does not. These results establish murine *bf* as a murine homologue to the yeast *vps33* mutant and suggest *VPS33A* as a candidate gene for some cases of human HPS.

Materials and Methods

Mice and Backcross. Mice carrying the spontaneous mutation *bf* on the C57BL/6J strain were obtained from The Jackson Laboratory and were subsequently bred at Roswell Park Cancer Institute. C57BL/6J *bf/bf* mice were crossed with the inbred, wild-derived *Mus musculus musculus* (PWK) inbred strain to obtain a high degree of polymorphism for molecular markers (9). A high-resolution genetic map of the *bf* critical region was generated by performing an interspecific cross between the *bf/bf* and PWK mice. At 6 weeks, 1,167 backcross progeny were typed for coat color and molecular markers by using microsatellite markers *D5Mit188* and *D5Mit212*, which flank *bf* proximally and distally, respectively. Informative mice were typed for 20 markers between *D5Mit188* and *D5Mit212*.

Phenotypic Analyses. Electron microscopy of mouse eyes (10), assays of platelet morphology and function (11), and assays of kidney and urine β-glucuronidase and β-galactosidase (12) were carried out as described. Platelet aggregation was determined by the impedance method in whole blood in response to 1 μg/ml collagen in *bf/bf* and C57BL/6J mice (11). ATP release was determined by luminescence methods.

Mutation Analyses. Overlapping amplicons spanning the coding regions of the mouse *Vps33a*, *Rnp24*, and *Atp6v0a2* genes and the murine homologues of human FLJ12975 and FLJ22471 were designed and used for RT-PCR amplification from mRNA of C57BL/6J and *bf/bf* mice. Kidney mRNA was prepared by using the RNeasy mini kit (Qiagen, Valencia, CA), and reverse transcription of total RNA was performed by using oligo dT primer and SuperScript II reverse transcriptase (GIBCO/BRL). Amplicons were screened for mutations by single-stranded conformational polymorphism/heteroduplex analysis (13), and a *Vps33a* amplicon, which showed an aberrant pattern, was reamplified and sequenced directly.

To screen for *VPS33A* mutations in human HPS patients, primers derived from intervening and noncoding sequences

Abbreviations: HPS, Hermansky–Pudlak syndrome; Vps, vacuolar protein sorting; bf, buff; car, carnation.

Data deposition: The sequences reported in this paper have been deposited in the GenBank database [accession nos. AF439858 (mouse *Vps33a* cDNA and amino acid sequences) and AF439857 (*VPS33A* cDNA and amino acid sequences)].

†T.S., N.O., and R.G. contributed equally to this work.

‡Present address: Department of Dermatology, Nagoya University School of Medicine, Showa-ku, Nagoya 466, Japan.

††To whom correspondence should be addressed. E-mail: richard.spritz@uchsc.edu.

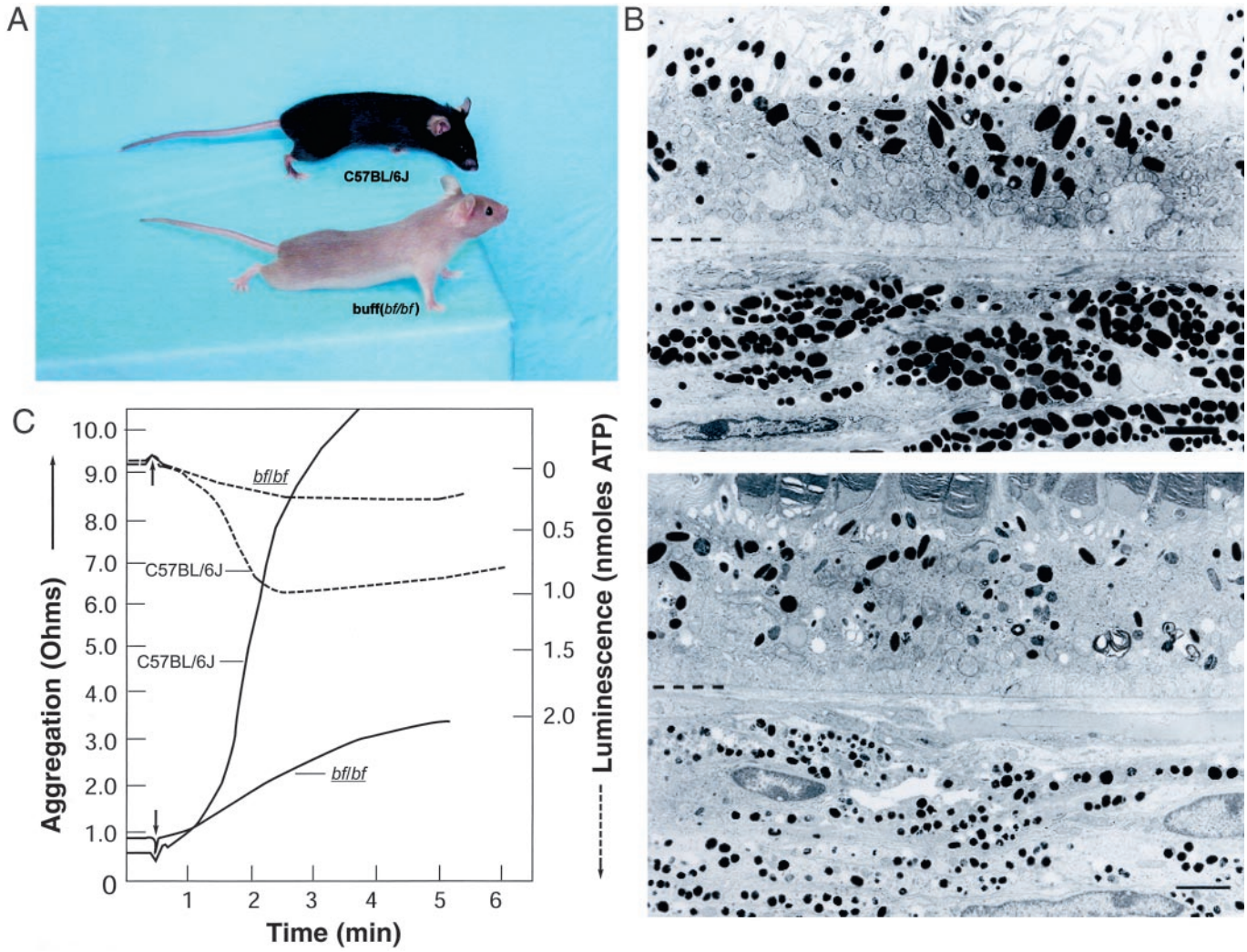

Fig. 1. Phenotype of *bf*-mutant mice. (*A*) Coat-color hypopigmentation in adult *bf*/*bf* versus C57BL/6J mice. (*B*) Reduced size and number of melanosomes in the eyes of *bf*/*bf* (*Lower*) versus wild-type C57BL/6J (*Upper*) mice. The dotted lines represent demarcation between retinal pigment epithelium (above) and choroid (below). (Scale bar, 2 μm.) (*C*) Reduced collagen-mediated platelet aggregation (solid line) and dense granule ATP secretion (dotted line) in *bf*/*bf* versus C57BL/6J mice. The arrows indicate the time of addition of collagen.

adjacent to the 13 genomic exons were used to amplify PCR products from genomic DNA of 26 HPS patients who lacked mutations in the *HPS1*, *HPS2* (*AP3B1*), *HPS3*, and *HPS4* loci. *VPS33A* amplicons were screened for mutations by single-stranded conformational polymorphism/heteroduplex analysis (13), and the one amplicon containing the Ile-256 → Leu variant was screened in DNA of 27 unrelated Puerto Rican controls.

Expression Plasmid Construction, Cell Culture, and Transformation. To construct *Vps33a* and *Vps33a*^{bf} expression plasmids, we first prepared full-length wild-type and Asp-251 → Glu mouse *Vps33a* cDNAs by nested RT-PCR using C57BL/6J and *bf*/*bf* mouse kidney cDNA, respectively, as described above and initial primers 5′-CGGGTGCCCGGGCAAGATG-3′/5′-GTGGTGACCTGTCACGTCTC-3′ and secondary primers 5′-GACTAGTGCCCCATGGCGGCGCACCTGTCGTACGG-3′ (containing an *Spe*I linker)/5′-CCGCTCGAGGTGGTGACCTGTCACGTCTCCTCCGA-3′ (containing an *Xho*I linker). The amplified cDNA fragments were cloned in pCR2.1 (Invitrogen) and sequenced to verify accuracy. The *Vps33a* and *Vps33a*^{bf} cDNAs were subcloned in-frame in the *Kpn*I and *Xho*I sites of GATEWAY pENTR3C (Invitrogen). The cDNAs then were transferred via site-specific recombination into pDEST26 (Invitrogen) and subsequently into the *Sna*BI and *Eco*RV sites of pIREShyg2 (CLONTECH).

Wild-type Melan-a (14) and Melan-bf (15) mouse melanocytes were cultured as described (10). Melan-bf cells were transfected with pIREShyg2-m*Vps33a*, pIREShyg2-m*Vps33a*^{bf}, and pIREShyg2 by using FuGENE 6 transfection reagent (Roche Diagnostics, Basel), and stably transformed cell lines were selected in medium containing 300 μg/ml hygromycin B (Invitrogen).

Results

Characterization of the *bf*-Mutant Phenotype. *bf* arose spontaneously in mice of the C57BL/6J strain (16) and is represented by a single mutant allele. Homozygous *bf*/*bf* mice exhibit reduced coat-color pigmentation (Fig. 1*A*). Lysosomal enzyme activities have been reported to be increased in kidneys of *bf* mice (17), although we have not been able to confirm these findings (see below). To characterize the *bf* phenotype further, we carried out electron microscopy of the eyes of *bf*/*bf* and C57BL/6J mice. As shown in Fig. 1*B*, melanosomes are markedly reduced in both size and number in the retinal pigment epithelium and choroid

GENETICS

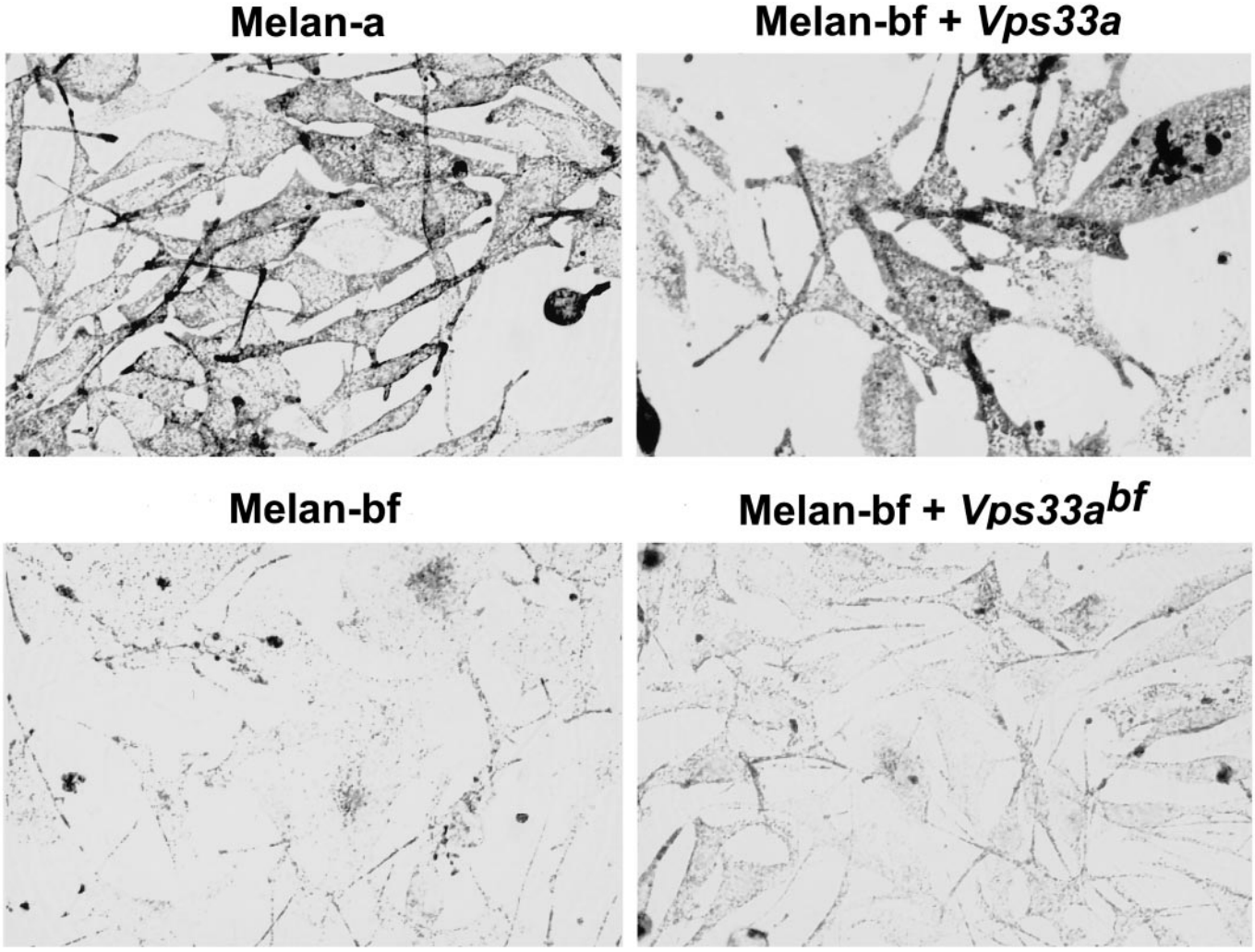

Fig. 2. Complementation of *bf*-mutant mouse melanocytes by *Vps33a*. Bright-field microscopy of wild-type (Melan-a) mouse melanocytes (14), *bf*-mutant (Melan-bf) mouse melanocytes (15), and *bf*-mutant melanocytes stably transformed by expression vectors containing wild-type (Melan-bf + Vps33a) or *bf*-mutant mouse *Vps33a* (Melan-bf + *Vps33a*^{bf}) cDNAs. Pigmented cytoplasmic granules are melanized melanosomes.

of *bf* mice. Similar findings were observed on analysis of a permanent line of mouse melanocytes derived from *bf*/*bf* mice (Fig. 2, Melan-bf) (15).

To assess platelet function in *bf* mice, we first tested bleeding time, which was prolonged significantly, to 9.7 ± 1.2 min in *bf*/*bf* homozygotes, versus 4.7 ± 0.7 min in *bf*/+ heterozygous controls ($P < 0.02$). Collagen-mediated platelet aggregation, secretion of dense-granule ATP (Fig. 1*C*), and platelet serotonin (not shown) all were reduced significantly in *bf*/*bf* mice. Furthermore, the number of dense granules per platelet, determined by whole-mount electron microscopy, was reduced greatly in *bf*/*bf* (5.07 ± 0.37) versus C57BL/6J (12.2 ± 0.79) mice ($P < 0.001$). These results establish that the *bf*-mutant phenotype includes significant platelet-storage pool defect, although this defect is less pronounced than in other mouse HPS-like mutants (6).

In contrast, we observed much less effect of the *bf* mutation on lysosomal enzyme activity and secretion. Kidney β-glucuronidase and β-galactosidase activities were not altered significantly in *bf*/*bf* versus C57BL/6J mice (not shown), and whereas secretion of β-galactosidase into urine was reduced by 53% ($P < 0.02$), the slight reduction we observed in β-glucuronidase secretion was not significant. Thus, the principal physiological effect of the *bf* mutation on organelles seems to be on melanosomes, with lesser effects on platelet-dense granules and little or no effect on lysosomes.

Fine Mapping and Identification of the Murine *bf* Locus. Mouse *bf* was mapped previously to 65.0 centimorgans on mouse chromosome 5, although not with high precision (18). To refine localization of the *bf* gene, we carried out a backcross of C57BL/6J mice homozygous for *bf* with mice of the PWK strain and typed 1,167 progeny for recombination events near *bf* using markers *D5Mit188* and *D5Mit282*, which flank *bf* proximally and distally, respectively. Fifty-six recombinant mice were then phenotyped for coat color and genotyped for 20 additional microsatellite markers previously mapped to this region of mouse chromosome 5: *D5Mit319*, *D5Mit368*, *D5Mit408*, *D5Mit137*, *D5Mit96*, *D5Mit160*, *D5Mit65*, *D5Mit369*, *D5Mit139*, *D5Mit279*, *D5Mit138*, *D5Mit95*, *D5Mit140*, *D5Mit161*, *D5Mit212*, *D5Mit244*, *D5Mit30*, *D5Mit162*, *D5Mit29*, and *D5Mit165*. These data localized *bf* to the 0.7-centimorgan interval between *D5Mit137* proximally and markers *D5Mit138*, *D5Mit139*, and *D5Mit279* distally; within this interval, four markers were nonrecombinant with *bf*: *D5Mit96*, *D5Mit160*, *D5Mit65*, and *D5Mit369*.

By analysis of the United Kingdom's Mouse Genome Centre database, we identified a sequence-tagged site within the *bf*

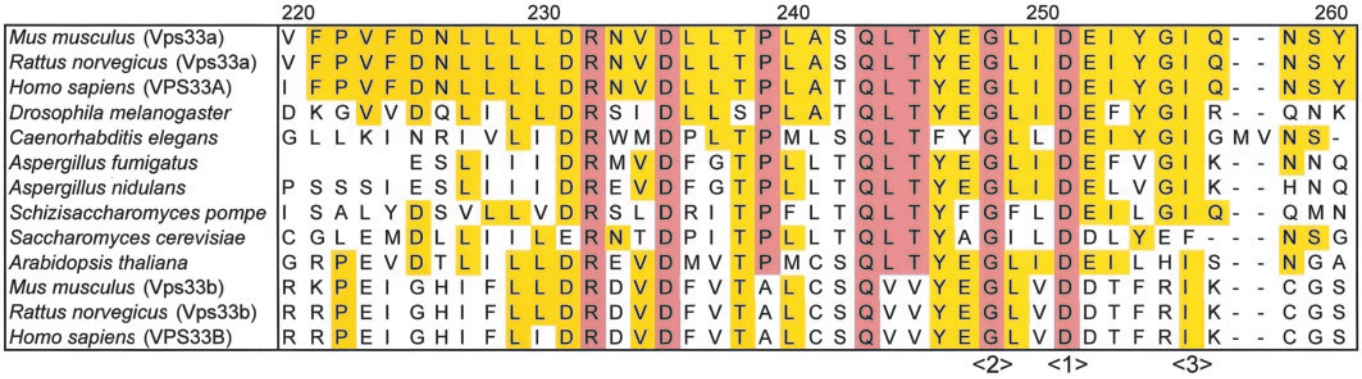

Fig. 3. Alignment of Vps33a-related amino acid sequences. Mouse Vps33a amino acid residues 220–260 are shown aligned to all known Vps33 orthologues and paralogues. Residues absolutely conserved among all available Vps33-related sequences (Vps33 unless indicated) are shown in red, and residues conserved among the three mammalian Vps33a paralogues are shown in yellow. <1>, mouse *Vps33a*^{bf} Asp-251 → Glu (GAT → GAG) substitution; <2>, *Drosophila car*^{1} Gly-249 → Val substitution (19); <3>, human *VPS33A* Ile-256 → Leu (ATT → CTT) substitution.

interval, AI120173, which represents a mouse orthologue of human *CD36L1*. This indicated that the *bf* region of mouse chromosome 5 is homologous to distal human chromosome 12q24. The NCBI and Celera human genome databases indicated that this region is ≈2.1 megabases in size, containing ≈71 known and predicted genes, of which *VPS33A*, *RNP24*, and *ATP6V0A2* had the greatest apparent biological relevance. We therefore screened for mutations in the mouse homologues of these three genes as well as the murine homologues of the predicted genes FLJ12975 and FLJ22471 by RT-PCR of kidney mRNA from *bf*/*bf* versus wild-type C57BL/6J mice and single-stranded conformational polymorphism/heteroduplex analysis (13) of the RT-PCR products. We detected an obvious abnormality in mouse *Vps33a*, and DNA sequence analyses of both the RT-PCR product and the genomic DNA defined a missense substitution of glutamic acid for aspartic acid at codon 251 (GAT → GAG). This substitution was not present in the wild-type C57BL/6J background on which the *bf* mutation arose. As shown in Fig. 3, Asp-251 has been conserved among all *Vps33* homologues for which sequences are available and is located only three residues distal to the glycine disrupted by the carnation (*car*) mutation of *Drosophila* (19).

Characterization and Complementation of Mouse *bf*-Mutant Melanocytes. To confirm that the *bf* gene is indeed *Vps33a*, we stably transformed a line of melanocytes derived from homozygous *bf*-mutant mice (15) by using both wild-type and *bf*-mutant (Asp-251 → Glu) *Vps33a* cDNAs. As shown in Fig. 2, *bf*-mutant melanocytes contain a reduced number of undermelanized melanosomes, which is similar to what is seen *in vivo* (Fig. 1*B*). Stable transformation by a vector expressing wild-type *Vps33a* cDNA completely complemented this abnormal phenotype, restoring normal melanosomal number and pigmentation (Fig. 2). In contrast, stable transformation by a plasmid expressing *bf*-mutant (Asp-251 → Glu) *Vps33a* cDNA or by the empty vector did not alter the mutant phenotype (Fig. 2). These results confirm that *Vps33a* is the mouse *bf* gene and that the Asp-251 → Glu substitution pathologically affects function of the Vps33a protein *in vivo*.

Analysis of *VPS33A* in Human Patients with HPS. We screened human *VPS33A* as a candidate HPS gene in 26 unrelated patients with HPS who lack mutations in the *HPS1*, *HPS2*, *HPS3*, and *HPS4* loci. One patient, of mixed Puerto Rican/Dominican origin, was found to be heterozygous for a missense substitution, Ile-256 → Leu (ATT → CTT). Ile-256 has been conserved among all known Vps33-related homologues (Fig. 3). Nevertheless, no other mutation was found in this patient. Although this substitution was not observed among 27 Puerto Rican controls, at present we cannot be certain whether this substitution has pathological significance or is a rare nonpathological polymorphism.

Discussion

Organelle biogenesis is a complex series of processes that organize trafficking of newly synthesized "cargo" proteins to the nascent organelles. In yeast, some 65 different genes have been implicated in biogenesis of the lysosome-like vacuole including >40 so-called *vps* loci required for assembly of the vacuolar ATPase and selective transport of certain soluble and membrane-bound proteins from the late Golgi/*trans*-Golgi network to the vacuole (7, 8). In mice and humans, fewer genes are known, but the diversity of organelles virtually assures that an even larger number of proteins are required for organellar biogenesis in mammals. The constellation of HPS-, Chediak–Higashi syndrome-, and Griscelli syndrome-like disorders of humans and mice indicates that melanosomes, lysosomes, and certain cytoplasmic granules share common pathways of organellar protein trafficking, although these pathways are as yet largely unknown. Here we have shown that the mouse *bf* locus corresponds to *Vps33a*, encoding a homologue of yeast *vps33*. This is the first mammalian mutant shown to involve a direct homologue of a classical yeast *vps* mutant, and the large amount known about protein trafficking to the yeast vacuole makes *bf* particularly instructive.

Vps33, a homologue of Sec1p-like regulators of membrane fusion, interacts with the Vps11, Vps16, Vps18, and probably also the Vps39 and Vps41 proteins to form the class C Vps complex (20), which in yeast is required for soluble *N*-ethylmaleimide-sensitive factor attachment protein receptor (SNARE)-mediated vesicle docking and fusion with the vacuole (21–23). Vps41, in turn, interacts with the AP-3 adaptor complex in a clathrin-independent pathway of vacuolar protein trafficking (24, 25). There is weak genetic interaction between *vps33* and a synthetic deletion of *apm3*, encoding the μ chain of AP-3 (26), although the nature of this interaction has not been defined. In *Drosophila*, the *car* eye color locus likewise corresponds to *vps33* (19), the *car*^{1} allele involving a Gly-249 → Val substitution, only three residues proximal to that homologous to Asp-251 in mouse Vps33A (Fig. 3).

In mammals (mouse, rat, and human), there are two *vps33* paralogues, *Vps33a* and *Vps33b* (27, 28), and the respective functions of the corresponding two Vps33-like proteins are not known. The relative specificity of the *bf*-mutant phenotype to

melanosomes and platelet granules versus virtual sparing of lysosomal function suggests that a Vps33a-containing class C Vps complex might be specifically involved in biogenesis of melanosomes and granules, whereas a Vps33b-containing class C Vps complex might be specifically involved in biogenesis of lysosomes. Because expression of both *Vps33a* and *Vps33b* seems to be ubiquitous (28, 29), any such functional specificity of these two Vps33-related proteins must reside at the protein level.

The identification of *Vps33a* as the murine *bf* locus suggests human *VPS33A* and perhaps also *VPS33B* as candidate HPS loci in man. Our data indicate that *VPS33A*, at least, is not a common HPS gene in humans. Nevertheless, rare cases of HPS may result from pathological mutations. The close functional association in yeast between the Vps33 protein and Vps11, Vps16, Vps18, Vps39, Vps41, and the AP-3 complex suggests these genes as additional candidates for the HPS-like loci of mouse and humans. Indeed, the mouse pearl (*pe*) and human *HPS2* loci have been found to correspond to *Ap3b1*, and the mouse mocha (*mh*) and *Drosophila* garnet (*g*) loci correspond to *Ap3d1* (2–4). Together, these findings strongly implicate a clathrin-independent AP-3 adaptor-class C Vps complex–soluble *N*-ethylmaleimide-sensitive factor attachment protein receptor pathway in mammalian melanosome, lysosome, and granule biogenesis.

We thank M. Reddington, S. Y. Jiang, L. Zhen, and D. Tabaczynski for expert technical assistance. This work was supported by National Institutes of Health Grants AR39892 (to R.A.S.), HL51480, HL31698, and EY12104 (to R.T.S.), and EY10199 (to P.G.S.), Roswell Park Cancer Institute Cancer Center Support Grant CA16056, and Welch Foundation Grant I-1300 (to P.G.S.).

1. Hermansky, F. & Pudlak, P. (1959) *Blood* **14,** 162–169.
2. Spritz, R. A. (1999) *Clin. Genet.* **55,** 309–317.
3. Spritz, R. A. (1999) *Trends Genet.* **15,** 337–340.
4. Spritz, R. A. (1999) *Pigm. Cell. Res.* **13,** 15–20.
5. Bennett, D. (1993) *Int. Rev. Cytol.* **146,** 191–260.
6. Swank, R. T., Novak, E. K., McGarry, M. P., Rusiniak, M. E. & Feng, L. (1998) *Pigm. Cell. Res.* **11,** 60–80.
7. Wendland, B., Emr, S. D. & Riezman, H. (1998) *Curr. Opin. Cell Biol.* **10,** 513–522.
8. Pelham, H. R. B. (1999) *Philos. Trans. R. Soc. London B* **354,** 1471–1478.
9. O'Brien, E. P., Novak, E. K., Keller, S. A., Poirier, C., Guenet, J. L. & Swank, R. T. (1994) *Mamm. Genome* **5,** 356–360.
10. Suzuki, T., Li., W., Zhang, Q., Novak, E. K., Sviderskaya, E. V., Wilson, A., Bennett, D. C., Roe, B. A., Swank, R. T. & Spritz, R. A. (2001) *Genomics* **78,** 30–37.
11. Swank, R. T., Sweet, H. O., Davisson, M. T., Reddington, M. & Novak, E. K. (1991) *Genet. Res.* **58,** 51–62.
12. Brandt, E. J., Elliott, R. W. & Swank, R. T. (1975) *J. Cell Biol.* **67,** 774–788.
13. Lee, S.-T., Park, S.-K., Lee, K.-H., Holmes, S. A. & Spritz, R. A. (1995) *Mol. Cells* **5,** 668–672.
14. Bennett, D. C., Cooper, P. J. & Hart, I. R. (1987) *Int. J. Cancer* **39,** 414–418.
15. Samaraweera, P., Donatien, P. D., Qazi, S., Kobayashi, T., Hearing, V. J., Panthier, J. J. & Orlow, S. J. (1999) *Eur. J. Biochem.* **266,** 924–934.
16. Dickie, M. M. (1964) *Mouse Newslett.* **30,** 30.
17. Hakansson, E. M. & Lundin, L. G. (1977) *Biochem. Genet.* **15,** 75–85.
18. Kerscher, S., Glenister, P. H., Favor, J. & Lyon, M. F. (1996) *Genomics* **36,** 17–21.
19. Sevrioukov, E. A., He, J.-P., Moghrabi, N., Sunio, A. & Kramer, H. (1999) *Mol. Cell* **4,** 479–486.
20. Rieder, S. E. & Emr, S. D. (1997) *Mol. Biol. Cell* **8,** 2307–2327.
21. Sato, T. K., Rehling, P., Peterson, M. R. & Emr, S. D. (2000) *Mol. Cell* **6,** 661–671.
22. Peterson, M. R. & Emr, S. D. (2001) *Traffic* **2,** 476–486.
23. Wurmser, A. E., Sato, T. K. & Emr, S. D. (2000) *J. Cell Biol.* **151,** 551–562.
24. Rehling, P., Darsow, T., Katzmann, D. J. & Emr, S. D. (1999) *Nat. Cell Biol.* **1,** 346–353.
25. Darsow, T., Katzmann, D. J., Cowles, C. R. & Emr, S. D. (2001) *Mol. Biol. Cell* **12,** 37–51.
26. Stepp, J. D., Huang, K. & Lemmon, S. K. (1997) *J. Cell Biol.* **139,** 1761–1774.
27. Pevsner, J., Hsu, S. C., Hyde, P. S. & Scheller, R. H. (1996) *Gene* **183,** 7–14.
28. Huizing, M., Didier, A., Walenta, J., Anikster, Y., Gahl, W. A. & Krämer, H. (2001) *Gene* **264,** 241–247.
29. Carim, L., Sumoy, L., Andreu, N., Estivill, X. & Escarceller, M. (2000) *Cytogenet. Cell Genet.* **89,** 92–95.